

Universality of Primordial Anisotropies in Gravitational Wave Background

Boyan Jiang¹, Ryo Saito^{2,3}, and Ying-li Zhang^{1,4,3,5}

¹ School of Physics Science and Engineering, Tongji University, Shanghai 200092, China
² Graduate School of Science and Engineering, Yamaguchi University, Yamaguchi 753-8512, Japan

³ Kavli Institute for the Physics and Mathematics of the Universe (WPI),
 UTIAS, The University of Tokyo, Chiba 277-8583, Japan

⁴ Institute for Advanced Study of Tongji University, Shanghai 200092, China and

⁵ Center for Gravitation and Cosmology, Yangzhou University, Yangzhou 225009, China

(Dated: February 9, 2026)

We propose a model-independent formalism for describing anisotropies in the stochastic gravitational wave background (SGWB) originating from primordial perturbations. Despite their diverse physical origins – such as Sachs–Wolfe effects, integrated Sachs–Wolfe effects, or fossil effects from primordial non-Gaussianity – SGWB anisotropies exhibit a universal angular structure. We show that this universality arises from a single vertex function, the Cosmological Form Factor (CFF), which encodes the information on how long-wavelength modes modulate the SGWB statistics. Two fundamental principles – statistical isotropy and locality – uniquely determine the angular dependence of the CFF, resulting in a universal multipole scaling of the SGWB anisotropies. The CFF formalism provides a common language for classifying SGWB anisotropies and offers a powerful framework for interpreting upcoming observations.

Introduction — The detection and characterization of the Stochastic Gravitational Wave Background (SGWB) represents one of the most promising frontiers in modern cosmology [1–3]. Unlike deterministic signals from compact binary coalescences, the SGWB arises from two types of stochastic contributions: (I) primordial perturbations generated by inflation and (II) a superposition of numerous unresolved sources. The type-I contributions – such as Primordial Gravitational Waves (PGWs) [4–6] and Scalar-Induced Gravitational Waves (SIGWs) [7–9] – are of particular interest, as they provide a direct window into the earliest moments of the universe and probe physics at energy scales far beyond the reach of terrestrial experiments.

Current theoretical frameworks predominantly assume that the SGWB is statistically homogeneous, isotropic, unpolarized and Gaussian, characterized completely by its spectral density $S_h(f)$ or the energy density $\Omega_{\text{GW}}(f)$ [1–3]. The current observational landscape spans multiple frequency decades, with different experimental techniques targeting complementary frequency ranges. At nanohertz frequencies, Pulsar Timing Arrays, notably NANOGrav [10], EPTA [11], PPTA [12], CPTA [13], and IPTA [14], have recently reported compelling evidence for a stochastic process consistent with the SGWB. While the current data cannot definitively distinguish between astrophysical and cosmological origins [15], the measured amplitude and spectral characteristics provide crucial constraints on early universe scenarios. Moving to higher frequencies, space-based interferometers such as LISA [16], Taiji [17], and TianQin [18] will probe the millihertz regime with unprecedented sensitivity. This frequency window is particularly promising for detecting the SIGWs, which are generated from large primordial curvature perturbations. The SIGWs provide a unique window into the primordial spectrum on scales far smaller than those accessible through cosmic microwave background

(CMB) measurements [19–23]. In particular, they offer a powerful probe for testing scenarios with enhanced small-scale perturbations, such as those leading to the formation of primordial black holes, which are a compelling candidate for dark matter [24–28]. At decihertz frequencies, DECIGO [29] aims to bridge the gap between space-based and ground-based detectors. While in the hectohertz to kilohertz band, ground-based interferometers (Advanced LIGO [30], Advanced Virgo [31], and KAGRA [32]) continue to improve their sensitivity to both astrophysical backgrounds and potential cosmological signals. The complementary nature of these observational windows allows us to distinguish between different production mechanisms.

However, as observational capabilities advance, a more complete statistical characterization is becoming increasingly essential [33]. While current analyses typically assume the SGWB to be statistically homogeneous, isotropic, unpolarized, and Gaussian, a variety of proposals have explored possible deviations from these standard assumptions [34–49]. Among these, we focus on the anisotropic features in the SGWB originating from primordial perturbations (Type I), which encode valuable information about the early universe. Despite their diverse physical origins, Type-I SGWB anisotropies exhibit a universal angular structure, whose physical origin has remained unexplained. In this work, we introduce a model-independent formalism – Cosmological Form Factor (CFF) – for describing Type-I SGWB anisotropies. We show that fundamental principles, statistical isotropy and locality, uniquely determine their angular structure, thereby explaining the universality in Type-I SGWB anisotropies. The CFF formalism not only clarifies the origin of the universality but also provides a common language for organizing diverse effects, offering a powerful framework for interpreting anisotropies in upcoming SGWB observations.

Angular Features of SGWB — The deviation from statistical isotropy is represented by the anisotropic power spectrum of GWs:

$$\langle h_\lambda^\dagger(\mathbf{q}) h_{\lambda'}(\mathbf{q}') \rangle = P_h(q) [1 + \delta_{\text{GW}}(q, \hat{\mathbf{q}})] \delta_{\lambda\lambda'} (2\pi)^3 \delta(\mathbf{q} - \mathbf{q}'), \quad (1)$$

where $h_\lambda^\dagger(\mathbf{q})$ denotes the Fourier mode with helicity $\lambda = \pm$, satisfying the reality condition $h_\pm^\dagger(\mathbf{q}) = h_\mp(-\mathbf{q})$. Here, we express the wave vector \mathbf{q} with its magnitude $q = |\mathbf{q}|$ and its unit direction $\hat{\mathbf{q}}$. Each mode $h_\pm(\mathbf{q})$ contains both positive- and negative-frequency components, which correspond to GWs coming from the direction $\hat{\mathbf{n}} = \hat{\mathbf{q}} (-\hat{\mathbf{q}})$ with frequency $f = q/2\pi (-q/2\pi)$ and polarization $\lambda = \pm (\mp)$, respectively. We adopt the circular polarization basis $e_{ij}^\pm(\hat{\mathbf{q}})$: they are related to the “plus-cross” polarization vectors as $e_{ij}^\pm(\hat{\mathbf{q}}) = e_{ij}^P(\hat{\mathbf{q}}) \pm i e_{ij}^C(\hat{\mathbf{q}})$ and thus satisfy $e_{ij}^\pm(-\hat{\mathbf{q}}) = e_{ij}^\mp(\hat{\mathbf{q}})$. The anisotropic power spectrum (1) induces angular dependence in the energy density as,

$$\Omega_{\text{GW}}(f) \rightarrow \Omega_{\text{GW}}(f)[1 + \delta_{\text{GW}}(f, \hat{\mathbf{n}})], \quad (2)$$

thereby encoding anisotropic features of the SGWB.

The statistical anisotropies can arise from several mechanisms, including:

- **Propagation effects** [36–39]:

Gravitational waves experience anisotropic distortions as they propagate through the inhomogeneous universe, analogous to Sachs-Wolfe (SW) and integrated Sachs-Wolfe (ISW) effects in the CMB.

- **Fossil effects (non-Gaussian effects)** [39–45]:

Mode couplings to cosmological-scale perturbations can imprint directional dependence in the initial SGWB statistics. This effect is especially pronounced in the presence of primordial non-Gaussianity, which couples modes of different scales.

The propagation-induced anisotropies are a universal feature of the SGWB and are not sensitive to specific scenarios. Importantly, such effects provide a valuable probe of the universe after inflation, offering insights into the matter distribution, cosmic expansion history, and large-scale gravitational potentials. In contrast, fossil signatures are model-dependent. While their presence is not guaranteed, they can serve as a powerful probe of inflationary physics and early-universe interactions beyond the simplest paradigms, especially in scenarios involving primordial non-Gaussianity.

The SGWB anisotropies can be characterized by the angular power spectrum,

$$\langle [\delta_{\text{GW}}]_{\ell m} [\delta_{\text{GW}}]_{\ell' m'} \rangle = \delta_{\ell\ell'} \delta_{mm'} C_\ell^{\text{GW}}, \quad (3)$$

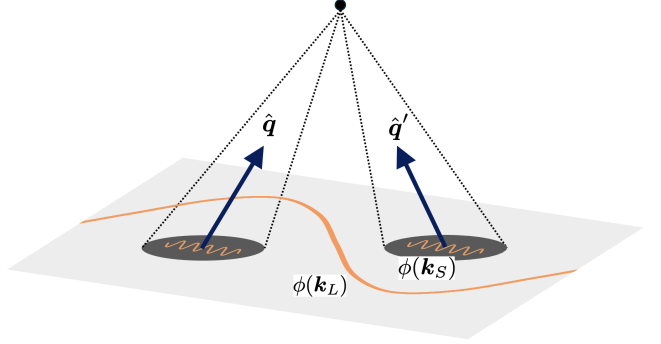


FIG. 1. Schematic illustration of the origin of SGWB anisotropies from long-wavelength perturbations. Gravitational waves observed in directions $\hat{\mathbf{q}}$ and $\hat{\mathbf{q}}'$ experience different local environments due to the presence of a long mode $\phi(\mathbf{k}_L)$, resulting in statistical anisotropies.

where $[\delta_{\text{GW}}]_{\ell m}$ denotes the spherical harmonic coefficients of the energy density contrast (2). Analogous to the CMB, the angular power spectrum C_ℓ^{GW} quantifies the statistical variance of the anisotropies as a function of angular scale. Intriguingly, C_ℓ^{GW} commonly exhibits a scaling behavior

$$C_\ell^{\text{GW}} \propto [\ell(\ell+1)]^{-1}, \quad (4)$$

regardless of the origins of the gravitational waves (PGWs or SIGWs) or the generation mechanism of the anisotropies (propagation or fossil effects) [36–45]. This work elucidates the origin of this universal scaling from general principles: symmetry and locality. We show that the ℓ -dependence naturally emerges from the fundamental statistical properties of the SGWB, providing a unified explanation across diverse scenarios.

Short-Long Modes Splitting — To reveal the universal structure underlying various mechanisms that generate the SGWB anisotropies, we consider observations of the sky with finite angular and frequency resolutions. In this situation, the observable quantity is described by a smoothed field defined with a window function W_Δ ,

$$[h_\lambda]_\Delta(\mathbf{q}) \equiv \int \frac{d^3 p}{(2\pi)^3} W_\Delta(|\mathbf{p} - \mathbf{q}|) h_\lambda(\mathbf{p}). \quad (5)$$

Our primary interest is how a primordial field ϕ , such as curvature perturbations, influences the statistical properties of the smoothed field (5). To this end, we split the primordial field ϕ into short-wavelength modes $\phi(\mathbf{k}_S)$ and long-wavelength modes $\phi(\mathbf{k}_L)$, which represent unresolvable and resolvable components, respectively (see Fig. 1). Hereafter, we also use the shorthand notations ϕ_S and ϕ_L . The presence of the long modes induces a bias in the statistics, thereby generating the statistical anisotropies (1) for the smoothed field. The impact of long modes on local observables is encoded in the conditional probability distribution $\mathbb{P}[h_\Delta | \phi_L]$, which describes

how the long modes ϕ_L modulate the statistics of the smoothed field h_Δ .

It is crucial to distinguish between two distinct averaging procedures. The smoothing (5), which corresponds to averaging over frequency bands and within a small sky patch, effectively performs an average over the short modes. We denote this by $\langle \cdot \rangle_S$. This *local* average probes the anisotropic power spectrum (1) for GWs originating from a specific direction and frequency range, and is determined by the conditional probability distribution $\mathbb{P}[h_\Delta|\phi_L]$ influenced by the long modes. In contrast, an average over the full sky corresponds to an average over the long modes. We denote this by $\langle \cdot \rangle_L$. This *global* average captures the angular power spectrum (3).

Cosmological Form Factor (CFF) — To characterize the anisotropic features induced by the long modes, we introduce an effective vertex $F_\lambda(\mathbf{q}, \mathbf{k}_L)$, referred to as the **Cosmological Form Factor (CFF)**, through

$$\langle |[h_\lambda]_\Delta(\mathbf{q})|^2 \rangle_S = P_h(q) N_\Delta \left[1 + \int \frac{d^3 k_L}{(2\pi)^3} F_\lambda(\mathbf{q}, \mathbf{k}_L) \phi(\mathbf{k}_L) \right], \quad (6)$$

where N_Δ is the normalization factor

$$N_\Delta \equiv \int \frac{d^3 p}{(2\pi)^3} |W_\Delta(|p|)|^2. \quad (7)$$

The CFF provides a universal description of how long modes bias the local statistics of SGWB at linear order, and is directly related to the SGWB anisotropy through

$$\delta_{\text{GW}}(q, \hat{\mathbf{q}}) = \int \frac{d^3 k_L}{(2\pi)^3} F_\lambda(\mathbf{q}, \mathbf{k}_L) \phi(\mathbf{k}_L). \quad (8)$$

Using the identity $\mathbb{P}[h_\Delta|\phi_L]\mathbb{P}[\phi_L] = \mathbb{P}[h_\Delta, \phi_L]$, we find the CFF is related to the bispectrum as,

$$F_\lambda(\mathbf{q}, \mathbf{k}_L) = \frac{\langle |[h_\lambda]_\Delta(\mathbf{q})|^2 \phi(\mathbf{k}_L) \rangle}{P_h(q) P_\phi(k_L) N_\Delta}, \quad (9)$$

where $\langle \cdot \rangle$ is an average over both the short and long modes. In the standard inflationary models, the full average $\langle \cdot \rangle$ respects the statistical isotropy. Hereafter, we investigate how the structure of the CFF is constrained by symmetry and locality.

Symmetry Constraint — The statistical isotropy of the bispectrum in Eq.(9) implies that the CFF can depend only on scalar combinations of the wavevectors. Accordingly, it must take the form

$$F_\lambda(\mathbf{q}, \mathbf{k}_L) = F(q, k_L, \hat{\mathbf{q}} \cdot \hat{\mathbf{k}}_L). \quad (10)$$

As already assumed in Eq.(10), the CFF is also independent of the GW polarization. A detailed derivation of this symmetry constraint will be presented in a companion paper.

Locality Constraint — The locality implies that the local statistics $\mathbb{P}[h_\Delta|\phi_L]$ can be biased only through the long

modes evaluated within a local sky patch. Thus, the relevant quantities are the long-mode field and its spatial derivatives,

$$\phi_L(\mathbf{x}, \tau_s), \nabla \phi_L(\mathbf{x}, \tau_s), \nabla \nabla \phi_L(\mathbf{x}, \tau_s), \dots \quad (11)$$

where \mathbf{x} denotes a position along the line of sight: $\mathbf{x} = \hat{\mathbf{q}}(\tau_0 - \tau_s)$. Here, τ_0 is the present conformal time and τ_s is the conformal time at which the corresponding anisotropy (or bias) is generated. From dimensional considerations, derivative terms are expected to be suppressed by factors of $k_L \tau_s$ or k_L/q . The smallness of $k_L \tau_s$ reflects the fact that the long modes are superhorizon at the source time τ_s . Compared with CMB observations, GW observations have lower angular resolution and probe earlier epochs, so that the long modes are well outside the horizon. This hierarchy ensures the validity of the derivative expansion implied by locality, justifying the truncation at the leading order. Taking the isotropy requirement (10) into account, the bias term in (6) must take the form

$$\int d\tau_s f(q, \tau_s) \phi_L(\mathbf{x}, \tau_s)|_{\mathbf{x}=\hat{\mathbf{q}}(\tau_0-\tau_s)}, \quad (12)$$

which implies

$$F(q, k_L, \hat{\mathbf{q}} \cdot \hat{\mathbf{k}}_L) = \int d\tau_s f(q, \tau_s) \mathcal{T}_\phi(k_L, \tau_s) e^{i(\hat{\mathbf{q}} \cdot \hat{\mathbf{k}}_L) k_L (\tau_0 - \tau_s)}. \quad (13)$$

Here, $\mathcal{T}_\phi(k_L, \tau_s)$ is the transfer function of the field ϕ . In conclusion, the symmetry and locality constraints uniquely determine the angular dependence of the CFF and, consequently, that of the SGWB anisotropy through Eq. (8).

Universal Scaling — Since the angular dependence of δ_{GW} has been uniquely determined, the angular power spectrum (3) can be written as,

$$C_\ell^{\text{GW}} = \int d\tau_s f(q, \tau_s) \mathcal{A}_\ell(\tau_s), \quad (14)$$

where

$$\mathcal{A}_\ell(\tau_s) \equiv \frac{2}{\pi} \int k_L^2 dk_L \mathcal{T}_\phi^2(k_L, \tau_s) P_\phi(k_L) j_\ell^2[k_L(\tau_0 - \tau_s)], \quad (15)$$

and j_ℓ denotes the ℓ -th spherical Bessel function. When the long modes are given by the curvature perturbations, their primordial power spectrum is nearly scale invariant on large scales relevant to the SGWB anisotropies: $P_\phi(k_L) \propto k_L^{-3}$. The transfer function $\mathcal{T}_\phi(k_L, \tau_s)$ is likewise scale independent, since the long modes remain superhorizon at the source time τ_s . Under these conditions, the ℓ -dependence of the angular power spectrum (14) is determined as

$$\mathcal{A}_\ell(\tau_s) \propto [\ell(\ell + 1)]^{-1}, \quad (16)$$

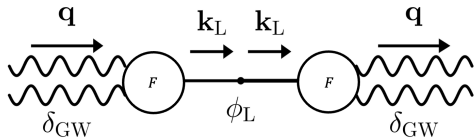


FIG. 2. Diagrammatic interpretation for the computation of the angular power spectrum (3) mediated by a single long mode. The CFF, $F(\mathbf{q}, \mathbf{k}_L)$, is represented by the vertices (circles) between the GW anisotropies δ_{GW} (double wavy lines) and the long modes ϕ_L (solid lines).

which yields the universal scaling behavior (4).

Extensions — While we have focused on scalar for the primordial field ϕ , our framework can be naturally extended to higher-spin fields. Tensor fields, for instance, would generate distinct angular patterns characterized by higher multipole moments [46–48]. The symmetry constraints become even more powerful in these cases, restricting the allowed angular and polarization structures of the CFF.

Our framework can be straightforwardly extended to higher orders in the long modes ϕ_L by introducing a separate form factor for each term in the expansion (6). To compute such higher-order contributions, it is convenient to adopt a diagrammatic approach. In this picture, each form factor plays the role of an effective vertex mediating the interaction between δ_{GW} and ϕ_L . For illustration, Fig. 2 shows the corresponding diagram for evaluating the angular power spectrum (3).

Conclusion and Outlook — In this work, we have introduced a systematic and model-independent framework for computing anisotropies in the SGWB induced by primordial perturbations on cosmological scales. The central object of this formalism is the Cosmological Form Factor (CFF), $F(\mathbf{q}, \mathbf{k}_L)$, which encodes how a long mode of cosmological perturbations with wavevector \mathbf{k}_L modulates the statistics of SGWB with wavevector \mathbf{q} . Although the detailed form of the CFF depends on the underlying production mechanism, symmetry and local

ity impose strong constraints on its angular structure. As a consequence, we have shown that a wide variety of physical processes give rise to the same multipole scaling of the SGWB anisotropies, $C_\ell \propto [\ell(\ell + 1)]^{-1}$, thereby explaining the universal behavior widely observed in the literature.

Our formalism demonstrates that a broad class of anisotropic effects, regardless of their microscopic origin, can be represented in a unified way through a single effective vertex described by the CFF. This provides not only a conceptual explanation for the similarity of SGWB anisotropy patterns across different scenarios, but also a classification scheme based on general principles. Moreover, the framework offers a practical pathway for distinguishing among different physical origins of SGWB anisotropies. It is notable that the CFF naturally retains information about the epoch at which the anisotropies are generated, through the source time τ_s . Cross-correlations with external cosmological probes – such as the CMB, galaxy surveys, or weak lensing – could therefore serve as powerful diagnostics to separate mechanisms that imprint anisotropies at different cosmic times [50–52].

Several natural extensions follow from our analysis. The CFF approach can be readily generalized to long modes with higher spin (*e.g.*, vector or tensor fields), as well as to higher-order effects (*e.g.*, loop corrections or non-Gaussian higher-point functions). We plan to explore these directions in forthcoming work.

In summary, our framework provides a general foundation for interpreting the anisotropic sky of gravitational waves and for extracting fundamental physics from future SGWB observations.

Acknowledgements — R.S. is supported by JSPS KAKENHI Grant Numbers JP23H01171 and JP23K25868, and Shanghai Sci-tech Co-research Program 25HB2700100. B.J. and Y.Z. are supported by the Fundamental Research Funds for the Central Universities, and by the Project 12475060 supported by NSFC, Project 24ZR1472400 sponsored by Natural Science Foundation of Shanghai, and Shanghai Pujiang Program 24PJA134.

[1] M. Maggiore, *Gravitational Waves. Vol. 1: Theory and Experiments* (Oxford University Press, 2007).

[2] C. Caprini and D. G. Figueira, *Class. Quant. Grav.* **35**, 163001 (2018), arXiv:1801.04268 [astro-ph.CO].

[3] N. Christensen, *Rept. Prog. Phys.* **82**, 016903 (2019), arXiv:1811.08797 [gr-qc].

[4] L. P. Grishchuk, *Zh. Eksp. Teor. Fiz.* **67**, 825 (1974).

[5] A. A. Starobinsky, *JETP Lett.* **30**, 682 (1979).

[6] V. A. Rubakov, M. V. Sazhin, and A. V. Veryaskin, *Phys. Lett. B* **115**, 189 (1982).

[7] K. N. Ananda, C. Clarkson, and D. Wands, *Phys. Rev. D* **75**, 123518 (2007), arXiv:gr-qc/0612013.

[8] D. Baumann, P. J. Steinhardt, K. Takahashi, and K. Ichiki, *Phys. Rev. D* **76**, 084019 (2007), arXiv:hep-th/0703290.

[9] G. Domènech, *Universe* **7**, 398 (2021), arXiv:2109.01398 [gr-qc].

[10] G. Agazie *et al.* (NANOGrav Collaboration), *Astrophys. J. Lett.* **951**, L8 (2023), arXiv:2306.16213 [astro-ph.HE].

[11] J. Antoniadis *et al.* (EPTA Collaboration), *Astronomy & Astrophysics* **678**, A50 (2023).

[12] A. Zic *et al.* (PPTA Collaboration), *Publications of the Astronomical Society of Australia* **40**, 10.1017/pasa.2023.36 (2023).

- [13] H. Xu *et al.* (CPTA Collaboration), *Research in Astronomy and Astrophysics* **23**, 075024 (2023).
- [14] G. Hobbs *et al.* (IPTA Collaboration), *Classical and Quantum Gravity* **27**, 084013 (2010).
- [15] A. Afzal *et al.* (NANOGrav Collaboration), *Astrophys. J. Lett.* **951**, L11 (2023), [Erratum: *Astrophys.J.Lett.* 971, L27 (2024), Erratum: *Astrophys.J.* 971, L27 (2024)], arXiv:2306.16219 [astro-ph.HE].
- [16] P. Auclair *et al.* (LISA Collaboration), *Living Reviews in Relativity* **26**, 5 (2023).
- [17] W.-H. Ruan *et al.* (Taiji Collaboration), *International Journal of Modern Physics A* **35**, 2050075 (2020).
- [18] E.-K. Li *et al.* (TianQin Collaboration), *Reports on Progress in Physics* **88**, 056901 (2025).
- [19] H. Assadullahi and D. Wands, *Phys. Rev. D* **81**, 023527 (2010), arXiv:0907.4073 [astro-ph.CO].
- [20] K. Kohri and T. Terada, *Phys. Rev. D* **97**, 123532 (2018), arXiv:1804.08577 [gr-qc].
- [21] R.-g. Cai, S. Pi, and M. Sasaki, *Phys. Rev. Lett.* **122**, 201101 (2019), arXiv:1810.11000 [astro-ph.CO].
- [22] C. T. Byrnes, P. S. Cole, and S. P. Patil, *JCAP* **06**, 028, arXiv:1811.11158 [astro-ph.CO].
- [23] K. Inomata and T. Nakama, *Phys. Rev. D* **99**, 043511 (2019), arXiv:1812.00674 [astro-ph.CO].
- [24] R. Saito and J. Yokoyama, *Phys. Rev. Lett.* **102**, 161101 (2009), [Erratum: *Phys.Rev.Lett.* 107, 069901 (2011)], arXiv:0812.4339 [astro-ph].
- [25] R. Saito and J. Yokoyama, *Prog. Theor. Phys.* **123**, 867 (2010), [Erratum: *Prog.Theor.Phys.* 126, 351–352 (2011)], arXiv:0912.5317 [astro-ph.CO].
- [26] E. Bugaev and P. Klimai, *Phys. Rev. D* **81**, 023517 (2010), arXiv:0908.0664 [astro-ph.CO].
- [27] J. Garcia-Bellido, M. Peloso, and C. Unal, *JCAP* **09**, 013, arXiv:1707.02441 [astro-ph.CO].
- [28] N. Bartolo, V. De Luca, G. Franciolini, M. Peloso, D. Racco, and A. Riotto, *Phys. Rev. D* **99**, 103521 (2019), arXiv:1810.12224 [astro-ph.CO].
- [29] S. Kawamura *et al.* (DECIGO collaboration), *Classical and Quantum Gravity* **28**, 094011 (2011).
- [30] J. Aasi *et al.* (Advanced LIGO Collaboration), *Classical and Quantum Gravity* **32**, 074001 (2015).
- [31] F. Acernese *et al.* (Advanced Virgo Collaboration), *Classical and Quantum Gravity* **32**, 024001 (2014).
- [32] T. Akutsu *et al.* (KAGRA Collaboration), *Nature Astronomy* **3**, 35–40 (2019).
- [33] J. D. Romano and N. J. Cornish, *Living Rev. Rel.* **20**, 2 (2017), arXiv:1608.06889 [gr-qc].
- [34] B. Allen, E. E. Flanagan, and M. A. Papa, *Phys. Rev. D* **61**, 024024 (2000), arXiv:gr-qc/9906054.
- [35] Z.-Y. Wu, R. Saito, and N. Sakai, *Phys. Rev. D* **107**, 023503 (2023), arXiv:2207.04669 [gr-qc].
- [36] C. R. Contaldi, *Phys. Lett. B* **771**, 9 (2017), arXiv:1609.08168 [astro-ph.CO].
- [37] N. Bartolo, D. Bertacca, S. Matarrese, M. Peloso, A. Ricciardone, A. Riotto, and G. Tasinato, *Phys. Rev. D* **100**, 121501 (2019), arXiv:1908.00527 [astro-ph.CO].
- [38] N. Bartolo, D. Bertacca, S. Matarrese, M. Peloso, A. Ricciardone, A. Riotto, and G. Tasinato, *Phys. Rev. D* **102**, 023527 (2020), arXiv:1912.09433 [astro-ph.CO].
- [39] J.-P. Li, S. Wang, Z.-C. Zhao, and K. Kohri, *JCAP* **06**, 039, arXiv:2309.07792 [astro-ph.CO].
- [40] N. Bartolo, D. Bertacca, V. De Luca, G. Franciolini, S. Matarrese, M. Peloso, A. Ricciardone, A. Riotto, and G. Tasinato, *JCAP* **02**, 028, arXiv:1909.12619 [astro-ph.CO].
- [41] E. Dimastrogiovanni, M. Fasiello, A. Malhotra, P. D. Meerburg, and G. Orlando, *JCAP* **02** (02), 040, arXiv:2109.03077 [astro-ph.CO].
- [42] E. Dimastrogiovanni, M. Fasiello, and L. Pinol, *JCAP* **09**, 031, arXiv:2203.17192 [astro-ph.CO].
- [43] Y.-H. Yu and S. Wang, *Phys. Rev. D* **109**, 083501 (2024), arXiv:2310.14606 [astro-ph.CO].
- [44] J.-P. Li, S. Wang, Z.-C. Zhao, and K. Kohri, *JCAP* **10**, 056, arXiv:2305.19950 [astro-ph.CO].
- [45] J.-P. Li, S. Wang, Z.-C. Zhao, and K. Kohri, arXiv e-prints , arXiv:2505.16820 (2025), arXiv:2505.16820 [astro-ph.CO].
- [46] A. Ricciardone and G. Tasinato, *JCAP* **02**, 011, arXiv:1711.02635 [astro-ph.CO].
- [47] E. Dimastrogiovanni, M. Fasiello, and G. Tasinato, *JCAP* **08**, 016, arXiv:1806.00850 [astro-ph.CO].
- [48] E. Dimastrogiovanni, M. Fasiello, and G. Tasinato, *Phys. Rev. Lett.* **124**, 061302 (2020), arXiv:1906.07204 [astro-ph.CO].
- [49] S. Akama, S. Hirano, and S. Yokoyama, *PTEP* **2025**, 103E01 (2025), arXiv:2410.14664 [astro-ph.CO].
- [50] P. Adshead, N. Afshordi, E. Dimastrogiovanni, M. Fasiello, E. A. Lim, and G. Tasinato, *Phys. Rev. D* **103**, 023532 (2021), arXiv:2004.06619 [astro-ph.CO].
- [51] A. Malhotra, E. Dimastrogiovanni, M. Fasiello, and M. Shiraishi, *JCAP* **03**, 088, arXiv:2012.03498 [astro-ph.CO].
- [52] M. Braglia and S. Kuroyanagi, *Phys. Rev. D* **104**, 123547 (2021), arXiv:2106.03786 [astro-ph.CO].